

The space–time domain: theory and modelling for anisotropic media

Tariq Alkhalifah,¹ Sergey Fomel² and Biondo Biondi²

¹The Institute for Astronomy and Geophysical Research, King AbdulAziz City of Science and Technology (KACST), Riyadh, Saudi Arabia. E-mail:tkhalfah@kacst.edu.sa

²Stanford Exploration Project (SEP), Stanford University, Palo Alto, CA, USA. E-mails: sergey@sep.stanford.edu; biondo@sep.stanford.edu

Accepted 2000 August 3. Received 2000 July 26; in original form 1999 December 23

SUMMARY

In transversely isotropic media with a vertical axis of symmetry (VTI media), we represent the image in vertical time, as opposed to depth, thus eliminating the inherent ambiguity of resolving the vertical P -wave velocity from surface seismic data. In this new $(x-\tau)$ -domain, the ray tracing and eikonal equations are completely independent of the vertical P -wave velocity, with the condition that the ratio of the vertical to normal-moveout (NMO) P -wave velocity (α) is laterally invariant. Moderate size departures of α from lateral homogeneity affect traveltimes only slightly. As a result, for all practical purposes, the VTI equations in the $(x-\tau)$ -domain become dependent on only two parameters in laterally inhomogeneous media: the NMO velocity for a horizontal reflector, and an anisotropy parameter, η . An acoustic wave equation in the $(x-\tau)$ -domain is also independent of the vertical P -wave velocity. It includes an asymmetric Laplacian operator to accommodate the unbalanced axis units in this new domain. In summary, we have established the basis for a full inhomogeneous time-processing scheme in VTI media that is dependent on only v and η , and independent of the vertical P -wave velocity.

Key words: anisotropy, modelling, traveltime.

INTRODUCTION

The main feature of the anisotropic parameter representation suggested by Alkhalifah & Tsvankin (1995) is that time processing—normal moveout (NMO) correction, dip moveout (DMO) and time migration—become independent of vertical P -wave velocity, a parameter necessary to resolve reflector depth. As a result, estimating the vertical velocity is unnecessary for time processing, which depends on only two parameters: the NMO velocity for a horizontal reflector and an anisotropy parameter denoted by η . However, this rather fortunate behaviour of seismic waves in transversely isotropic media with a vertical symmetry axis (VTI media) seems to hold only for vertically inhomogeneous media. When lateral inhomogeneity exists, three parameters are needed to characterize the medium and implement processing.

Our goal is to implement time processing that truly honours the lateral inhomogeneity of the medium and yet is independent of the vertical P -wave velocity. Separating the P -wave vertical velocity, v_v , from the image processing procedure helps to avoid the intrinsic ambiguity that this velocity introduces into the problem of estimating parameters in VTI models. This separation allows us to correct for the depth whenever such information becomes available, for example from well-log data.

This report shows that certain lateral inhomogeneities fall into this fortunate category of independence from vertical P -wave velocity when we replace the depth axis with the vertical time. We refer to such an inhomogeneity as being *factorized laterally*. The term *factorized* was introduced by Shearer & Chapman (1988) to describe a medium in which the ratio between the different elastic coefficients remains constant throughout the medium. In the case of our new coordinate system, this constraint is needed only between the P -wave NMO velocity and vertical velocity and it is needed only laterally. In other words, α , defined as the ratio between the vertical and NMO P -wave velocities, can change only vertically. This condition still allows for data processing in media of any lateral inhomogeneity, but does not allow for applying any depth conversion. In fact, this condition is extremely convenient considering that reflector depth is typically resolved at only one location along a given seismic line (at the well), and that we can therefore use this $\alpha(z)$, extracted from the well, to estimate depths. When α varies laterally, the accuracy of the processing depends on the size of the variation. Our analysis shows that such a dependence is small for typical variations and, as a result, can be ignored.

The term *time processing* implies that an image of the subsurface is obtained with its vertical axis given in time rather

than in depth. Traditionally, only vertical inhomogeneity is treated in time processing. Such processing might include approximations to treat mild inhomogeneities, but nothing that could come close to properly imaging complex data such as the Marmousi model. *Time processing* takes on a quite different meaning in this paper. It includes exact treatment for media with any lateral inhomogeneity. Specifically, we develop ray-theoretical solutions of wave propagation in the time domain, including the eikonal and ray-tracing equations that can handle any lateral inhomogeneity. An acoustic wave equation constrains all other aspects (such as amplitudes) of wave propagation in the $(x-\tau)$ -domain. We also show numerical results of ray tracing and examine its dependence on only two parameters in VTI media.

PARAMETRIZATION IN ANISOTROPIC MEDIA

In homogeneous transversely isotropic media with a vertical symmetry axis (VTI media), P and SV waves (we omit the qualifiers in *quasi-P* and *quasi-SV waves* for brevity) can be described by the vertical velocities V_{P0} and V_{S0} of P and S waves, respectively, and two dimensionless parameters ε and δ (Thomsen 1986). Tsvankin & Thomsen (1994) and Alkhalifah (1998) demonstrated that P -wave velocity and traveltime are practically independent of V_{S0} , even for strong anisotropy. Thus, for practical purposes, P -wave kinematic signatures can be considered as a function of just three parameters: V_{P0} , δ and ε .

Alkhalifah & Tsvankin (1995) further demonstrated that a new representation in terms of just two parameters is sufficient for performing all time-related processing such as NMO correction (including non-hyperbolic moveout correction, if necessary), dip-moveout removal and pre- and post-stack time migration, assuming that the velocity varies only vertically. These two parameters are the NMO velocity for a horizontal reflector,

$$V_{\text{nmo}}(0) = V_{P0} \sqrt{1 + 2\delta}, \quad (1)$$

and the anisotropy coefficient,

$$\eta \equiv 0.5 \left(\frac{V_h^2}{V_{\text{nmo}}^2(0)} - 1 \right) = \frac{\varepsilon - \delta}{1 + 2\delta}, \quad (2)$$

where V_h is the horizontal velocity. Instead of V_{nmo} , we use v to denote the interval NMO velocity in both isotropic and TI media.

THE DEPTH ISSUE

The depth axis has always been a source of uncertainty in seismic processing. Geophysicists have shied away from predicting depths from surface seismic P -wave data. Typically, well-log data are used for such a task. However, since well-log data are rare and sparse, seismically based interpolations of well-log information are commonly used. Although the conventional isotropic theory suggests that depth can be resolved using the velocity field that focuses the seismic image, field data have rarely agreed with this isotropic principal. Anisotropy, on the other hand, suggests that depth cannot be resolved using surface seismic data. The velocity needed to resolve depth is the vertical velocity, which is different from the imaging velocity

(the velocity that yields the best image). This difference is in agreement with typical field data experience. In fact, in VTI media, processing is controlled by three velocities: one responsible for *depthing*, another for *stacking* and the third for *migration*. Although this is a simplistic representation and theory suggests that there is more interaction between these velocities and their influences, such a representation is close to what actually happens in practice. Two of these velocities are resolvable from surface seismic data, or, in a general inhomogeneous case, two combinations of these velocities are resolvable, which implies the existence of a null space in the three-parameter representation of VTI media.

Considering that depth in VTI media is determined by multiplying half of the vertical traveltime by the vertical velocity, it seems that representing data with the vertical time, instead of depth, can absorb the vertical velocity influence. This has been shown to be the case for vertically inhomogeneous media (Alkhalifah & Tsvankin 1995) but has yet to be shown for more general inhomogeneity. In the next section, we replace the depth axis with vertical time to represent more general, arbitrarily inhomogeneous media.

REPRESENTING DEPTH WITH VERTICAL TIME

In this section, we derive the relation between the depth and the vertical time axis for a general inhomogeneous medium. Using this relation, the VTI eikonal equation is represented in the new $(x-\tau)$ -domain coordinate system. Hatton *et al.* (1981) implemented a similar mapping to show the limitations of time migration in isotropic media.

Two-way vertical time is related to depth by the following relation:

$$\tau(x, z) = \int_0^z \frac{2}{v_v(x, \zeta)} d\zeta, \quad (3)$$

where v_v is the vertical P -wave velocity, which can vary vertically as well as laterally. As follows from eq. (3), the stretch applied to the depth axis varies laterally.

Alkhalifah (2000) derived a simple form of the eikonal equation for VTI media, based on setting the shear wave velocity to zero. For 2-D media it is

$$v^2 (1 + 2\eta) \left(\frac{\partial t}{\partial x} \right)^2 + v_v^2 \left(\frac{\partial t}{\partial z} \right)^2 \left[1 - 2v^2 \eta \left(\frac{\partial t}{\partial x} \right)^2 \right] = 1. \quad (4)$$

This equation, based on the acoustic medium assumption in VTI media, although not physically possible, yields extremely accurate traveltime solutions that are close to what we obtain for the conventional elastic media equations.

The eikonal equation includes first-order derivatives of traveltime with respect to position. In order to transform this eikonal equation from the depth to the time coordinate, we need to replace x with \tilde{x} . Using the chain rule, $\partial t / \partial x$ in eq. (4) is given by

$$\frac{\partial t}{\partial x} = \frac{\partial t}{\partial \tilde{x}} + \frac{\partial t}{\partial \tau} \sigma, \quad (5)$$

where σ , extracted from eq. (3), is written as

$$\sigma(x, z) = \frac{\partial \tau}{\partial x} = \int_0^z \frac{\partial}{\partial x} \left(\frac{2}{v_v(x, \zeta)} \right) d\zeta. \quad (6)$$

Likewise, the partial derivative in z in the eikonal equation is

$$\frac{\partial t}{\partial z} = \frac{2}{v_v} \frac{\partial t}{\partial \tau}. \quad (7)$$

Therefore, the transformation from (x, z) to (\tilde{x}, τ) is governed by the following Jacobian matrix in 2-D media:

$$\mathbf{J} = \begin{pmatrix} 1 & \sigma \\ 0 & \frac{2}{v_v} \end{pmatrix}. \quad (8)$$

Substituting eqs (5) and (7) into the eikonal eq. (4) yields

$$v^2 (1 + 2\eta) \left(\frac{\partial t}{\partial \tilde{x}} + \frac{\partial t}{\partial \tau} \sigma \right)^2 + 4 \left(\frac{\partial t}{\partial \tau} \right)^2 \left[1 - 2v^2 \eta \left(\frac{\partial t}{\partial \tilde{x}} + \frac{\partial t}{\partial \tau} \sigma \right)^2 \right] = 1, \quad (9)$$

which is indirectly independent of the vertical velocity. However, according to eq. (6), σ still depends on the vertical P -wave velocity. Rewriting eq. (6) in terms of the two-way vertical time (see Appendix A) gives us

$$\sigma(\tilde{x}, \tau) = \frac{-1}{v_v(\tilde{x}, \tau)} \int_0^\tau \frac{\partial v_v(\tilde{x}, \tilde{\tau})}{\partial \tilde{x}} d\tilde{\tau}, \quad (10)$$

where \tilde{x} corresponds to the new coordinates (\tilde{x}, τ) . In the case of $v_v(x, z) = \alpha(z)v(x, z)$, which is a special case of lateral inhomogeneity, referred to here as *laterally factorized*, eq. (6) takes the form

$$\sigma(x, \tau) = \int_0^\tau \frac{\partial}{\partial x} \left(\frac{1}{v} \right) v d\tilde{\tau}, \quad (11)$$

which is clearly independent of the vertical P -wave velocity. Also, eq. (10) becomes

$$\sigma(\tilde{x}, \tau) = \frac{-1}{v(\tilde{x}, \tau)} \int_0^\tau \frac{\partial v(\tilde{x}, \tilde{\tau})}{\partial \tilde{x}} d\tilde{\tau}. \quad (12)$$

The eikonal equation can be used to compute seismic travel-times in laterally factorized inhomogeneous media without the need to estimate the vertical P -wave velocity. The departure of the medium from this special condition of laterally factorized media will cause errors in traveltimes calculation. We can estimate these errors by evaluating how much σ varies between eqs (6) and (11). Specifically, if $v_v(x, z) = \alpha(x, z)v(x, z)$, then

$$\Delta\sigma(x, \tau) = \int_0^\tau \frac{\partial}{\partial x} \left(\frac{1}{\alpha} \right) d\tilde{\tau}. \quad (13)$$

If the ratio of the vertical to NMO velocity, α , does not change laterally, $\Delta\sigma$ is equal to zero, and thus no errors will occur in the traveltimes calculation. The departure of $\Delta\sigma$ from zero affects only the x -axis component of the wave front; according to eqs (5) and (7) it is only $\partial t / \partial x$ that depends on σ . The vertical component of the traveltimes remains accurate no matter how much α varies laterally. Also, because the eikonal equation is independent of σ for horizontally travelling waves ($\partial t / \partial \tau = 0$), such waves are error-free. The majority of the errors caused by lateral α variation occur around 45° wave propagation.

In terms of VTI parameters, the NMO velocity is given by (Thomsen 1986)

$$v(x, z) = v_v(x, z) \sqrt{1 + 2\delta(x, z)}.$$

Therefore,

$$\alpha(x, z) = \frac{1}{\sqrt{1 + 2\delta(x, z)}}$$

and

$$\frac{d}{dx} \frac{1}{\alpha} = \frac{1}{[1 + 2\delta(x, z)]^{1/2}} \frac{d\delta}{dx} \approx \frac{d\delta}{dx}.$$

Then

$$\Delta\sigma \approx \int_0^\tau \frac{d\delta}{dx} d\tilde{\tau}.$$

We can see that the absolute error, resulting from the integral formulation, clearly increases with time.

In addition, when we use the new coordinate system (x, τ) , the transport equation becomes independent of the vertical velocity under the same condition of laterally factorized media (see Appendix B). Below, and for simplicity, we will replace \tilde{x} with x to denote the lateral coordinate in the new coordinate system.

RAY-TRACING EQUATIONS

Using the method of characteristics, we can derive a system of ordinary differential equations that define the ray trajectories. To do so, we need to transform eq. (9) to the following form:

$$F\left(x, \tau, \frac{\partial t}{\partial x}, \frac{\partial t}{\partial \tau}\right) = 0 \quad (14)$$

or

$$F(x, \tau, p_x, p_\tau) = 0, \quad (15)$$

where $p_x = \partial t / \partial x$ and $p_\tau = \partial t / \partial \tau$. According to the classic rules of mathematical physics (Courant & John 1966), the solutions of this kinematic equation can be obtained from the system of ordinary differential equations,

$$\begin{aligned} \frac{dx}{ds} &= \frac{1}{2} \frac{\partial F}{\partial p_x}, & \frac{d\tau}{ds} &= \frac{1}{2} \frac{\partial F}{\partial p_\tau}, \\ \frac{dp_x}{ds} &= -\frac{1}{2} \frac{\partial F}{\partial x}, & \frac{dp_\tau}{ds} &= -\frac{1}{2} \frac{\partial F}{\partial \tau}, \end{aligned} \quad (16)$$

where s is a running parameter along the rays, related to the traveltimes t as follows:

$$\frac{dt}{ds} = \frac{1}{2} p_\tau \frac{\partial F}{\partial p_\tau} + p_x \frac{\partial F}{\partial p_x},$$

with

$$\begin{aligned} \frac{dx}{dt} &= \frac{dx/ds}{dt/ds}, & \frac{d\tau}{dt} &= \frac{d\tau/ds}{dt/ds}, \\ \frac{dp_x}{dt} &= \frac{dp_x/ds}{dt/ds}, & \frac{dp_\tau}{dt} &= \frac{dp_\tau/ds}{dt/ds}. \end{aligned} \quad (17)$$

Using eq. (9), we obtain

$$\frac{dx}{ds} = av^2 [1 + 2\eta(1 - 4p_\tau^2)], \quad (18)$$

$$\frac{d\tau}{ds} = 4p_\tau - av^2 [-\sigma + 2\eta(-\sigma + 4p_x p_\tau + 8\sigma p_\tau^2)], \quad (19)$$

$$\begin{aligned} \frac{dp_x}{ds} = & -a^2 v [1 + 2\eta(1 - 4p_\tau^2)] v_x \\ & - av^2 [a(1 - 4p_\tau^2)\eta_x + p_\tau(1 + 2\eta - 8\eta p_\tau^2)\sigma_x], \end{aligned} \quad (20)$$

$$\begin{aligned} \frac{dp_\tau}{ds} = & -va^2 [1 + 2\eta(1 - 4p_\tau^2)] v_\tau \\ & - v^2 a [a(1 - 4p_\tau^2)\eta_\tau + p_\tau(1 + 2\eta - 8\eta p_\tau^2)\sigma_\tau] \end{aligned} \quad (21)$$

and

$$\frac{dt}{ds} = 4p_\tau^2 + a^2 v^2 [1 + 2\eta(1 - 8p_\tau^2)],$$

where

$$a = p_x + \sigma p_\tau,$$

and $v_x = \partial v / \partial x$ and $v_\tau = \partial v / \partial \tau$, and the same holds for η and σ .

To trace rays, we must first identify the initial values x_0 , τ_0 , p_{x0} and $p_{\tau 0}$. The variables x_0 and τ_0 describe the source position, and p_{x0} and $p_{\tau 0}$ are extracted from the initial take-off angle of propagation. Note that, from eq. (9),

$$p_{\tau 0} = 1 - \frac{v^2 p_{x0}^2}{1 - 2\eta v^2 p_{x0}^2},$$

because $\sigma = 0$ at the source position ($z = 0$).

The ray-tracing system of equations (18)–(21) describes the ray-theoretical aspect of wave propagation in the $(x-\tau)$ -domain, and can be used as an alternative to the eikonal equation. Numerical solutions of the ray-tracing equations, as opposed to the eikonal equation, provide multi-arrival traveltimes and amplitudes. In the numerical examples, we use ray tracing to highlight some of the features of the $(x-\tau)$ -domain coordinate system.

THE $x-\tau$ ACOUSTIC WAVE EQUATION

Following the approach of Alkhalifah (2000), an acoustic wave equation is simply derived from the eikonal equation using Fourier transformations. The addition of σ results in a more intriguing wave equation than the one derived by Alkhalifah (2000). Instead of the symmetric form of the familiar Laplacian in isotropic media, two sources of asymmetry are introduced into the new wave equation. One is caused by the new unbalanced coordinate system with one axis given in time and the other in position. The second, caused by anisotropy, is similar to that described by Alkhalifah (2000).

Using $k_x = \omega \partial t / \partial x$ and $k_\tau = \omega \partial t / \partial \tau$, where k_x is the horizontal component of the wavenumber vector, k_τ is the vertical-time-normalized component of the wavenumber vector (normalized by the vertical velocity, thus it has frequency units) and ω is the angular frequency, we can transform eq. (9) into

$$\begin{aligned} v^2 (1 + 2\eta) \left(\frac{k_x}{\omega} + \frac{k_\tau}{\omega} \sigma \right)^2 \\ - 4 \left(\frac{k_\tau}{\omega} \right)^2 \left[1 - 2v^2 \eta \left(\frac{k_x}{\omega} + \frac{k_\tau}{\omega} \sigma \right)^2 \right] = 1. \end{aligned} \quad (22)$$

Multiplying both sides of eq. (22) by the wavefield in the Fourier domain, $F(k_x, k_\tau, \omega)$, as well as using inverse Fourier transform on k_τ , k_x and ω ($k_\tau \rightarrow -i\partial/\partial\tau$, $k_x \rightarrow -i\partial/\partial x$ and $\omega \rightarrow i\partial/\partial t$), we obtain the acoustic wave equation in this new vertical-velocity-independent coordinate system,

$$\begin{aligned} \frac{\partial^4 F}{\partial t^4} = & -8 \frac{\partial^4 F}{\partial x^2 \partial \tau^2} v^2 \eta + \frac{\partial^4 F}{\partial x^2 \partial t^2} v^2 (1 + 2\eta) \\ & - 16 \frac{\partial^4 F}{\partial x \partial \tau^3} v^2 \eta \sigma + 2 \frac{\partial^4 F}{\partial t^2 \partial x \partial \tau} v^2 (1 + 2\eta) \sigma \\ & - 8 \frac{\partial^4 F}{\partial \tau^4} v^2 \eta \sigma^2 + \frac{\partial^4 F}{\partial t^2 \partial \tau^2} [4 + v^2 (1 + 2\eta) \sigma^2]. \end{aligned} \quad (23)$$

This equation is a fourth-order partial differential equation. Unlike the acoustic wave equation of Alkhalifah (2000) for VTI media, eq. (23) has odd-order derivatives caused by the asymmetry of the coordinate system. Setting $\sigma = 0$ [$dx/dx = 0$], we obtain a similar equation to that of Alkhalifah, with ∂z replaced by $v_\tau \partial \tau$ as follows:

$$\frac{\partial^4 F}{\partial t^4} = -8 \frac{\partial^4 F}{\partial x^2 \partial \tau^2} v^2 \eta + \frac{\partial^4 F}{\partial x^2 \partial t^2} v^2 (1 + 2\eta) + 4 \frac{\partial^4 F}{\partial t^2 \partial \tau^2}. \quad (24)$$

Setting $\eta = 0$ in eq. (23) yields the acoustic equation for elliptically anisotropic media in the $(x-\tau)$ -domain,

$$\frac{\partial^2}{\partial t^2} \left[\frac{\partial^2 F}{\partial t^2} - v^2 \left(\frac{\partial^2 F}{\partial x^2} + 2 \frac{\partial^2 F}{\partial x \partial \tau} \sigma \right) - \frac{\partial^2 F}{\partial \tau^2} (4 + v^2 \sigma^2) \right] = 0. \quad (25)$$

Substituting $P = \partial^2 F / \partial t^2$, we obtain the second-order wave equation for elliptically anisotropic media,

$$\frac{\partial^2 P}{\partial t^2} = v^2 \left(\frac{\partial^2 P}{\partial x^2} + 2 \frac{\partial^2 P}{\partial x \partial \tau} \sigma \right) + \frac{\partial^2 P}{\partial \tau^2} (4 + v^2 \sigma^2). \quad (26)$$

Rewriting eq. (23) in terms of $P(x, y, z, t)$ rather than $F(x, y, z, t)$ wherever possible yields

$$\begin{aligned} \frac{\partial^2 P}{\partial t^2} = & -8 \frac{\partial^4 F}{\partial x^2 \partial \tau^2} v^2 \eta + \frac{\partial^2 P}{\partial x^2} v^2 (1 + 2\eta) \\ & - 16 \frac{\partial^4 F}{\partial x \partial \tau^3} v^2 \eta \sigma + 2 \frac{\partial^2 P}{\partial x \partial \tau} v^2 (1 + 2\eta) \sigma \\ & - 8 \frac{\partial^4 F}{\partial \tau^4} v^2 \eta \sigma^2 + \frac{\partial^2 P}{\partial \tau^2} [4 + v^2 (1 + 2\eta) \sigma^2], \end{aligned} \quad (27)$$

where

$$F(x, y, z, t) = \int_0^t dt' \int_0^{t'} P(x, y, z, \tau) d\tau.$$

Because of its second-order nature in time, eq. (27) is simpler to use in a numerical implementation than eq. (23). The acoustic wave equation in the $(x-\tau)$ -domain is clearly independent of the vertical velocity when σ is given by eq. (12) and α is laterally invariant.

NUMERICAL EXAMPLES

Using the ray-tracing system of equations (18)–(21), we can compute traveltimes numerically. Unlike numerical solutions of the eikonal equation, ray tracing provides multi-arrival traveltimes and amplitudes. In this section, we want to confirm numerically two features of implementing ray tracing in the new coordinate system:

- (i) the traveltime solution when transformed to depth agrees with results from conventional depth-domain ray tracing;
- (ii) the traveltime solution in the $(x-\tau)$ -domain is independent of the vertical P -wave velocity for media that are factorized laterally [$\partial\alpha/\partial x=0$].

Fig. 1 shows two sets of 16 rays originating from a source on the surface at position $x=0$ through the same depth-velocity model of $v_v(x, z)=1.5+0.225z+0.15x$, $v(x, z)=2.0+0.3z+0.2x$ and $\eta(x, z)=0.1+0.05z+0.05x$ using conventional ray tracing in the depth domain (black curves), and the new ray tracing in the $(x-\tau)$ -domain (grey curves). We achieved the $(x-\tau)$ -domain ray-tracing results by mapping the depth velocity model to time using eq. (3) and then mapping the ray solutions back to depth using eq. (A2) after ray tracing. The 16 rays have ray parameters ranging from zero to the maximum value of $1/V_h$ (V_h is the horizontal velocity), with a fixed ray-parameter spacing of $1/(15V_h)$. The rays terminate at the same time of 8 s, and the wave fronts (given by the dashed curves) are plotted at about 1.6 s intervals. The wave fronts that correspond to the different ray tracings are virtually coincident, a result that agrees with our analytical findings.

In Fig. 2, we check for another aspect of the theory, that is, the independence of ray tracing from the vertical velocity for laterally factorized VTI media. Again, 16 rays were ray traced through a VTI model with $v(x, z)=2+0.2x$ km s⁻¹ and $\eta(x, z)=0.1+0.05z+0.05x$. The ray tracing was performed

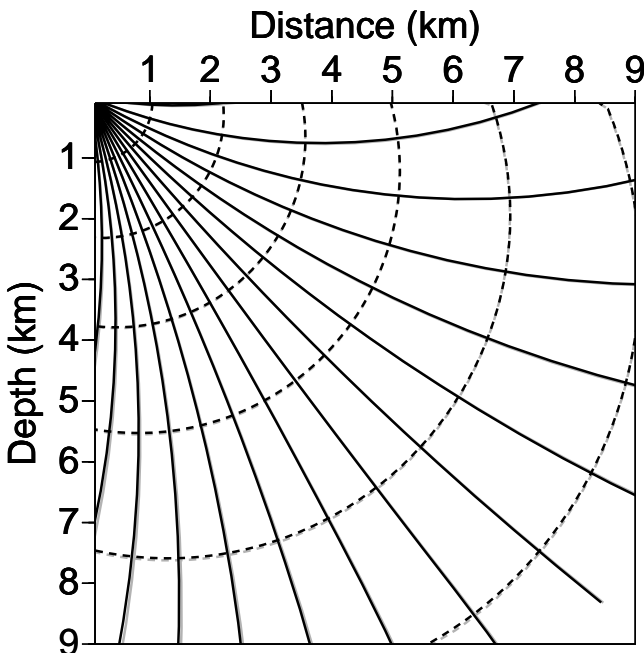


Figure 1. Ray paths (solid curves) and corresponding wave fronts (dashed curves) for an inhomogeneous VTI model with $v(x, z)=2.0+0.3z+0.2x$ km s⁻¹, $v_v(x, z)=1.5+0.225z+0.15x$ km s⁻¹ and $\eta(x, z)=0.1+0.05z+0.05x$. The black curves are obtained through conventional ray tracing in the depth domain, and the grey curves are obtained using the equivalent $(x-\tau)$ -domain ray tracing, where the results are ultimately converted to depth. In this case, the curves nearly overlap; they are only barely distinguishable, which agrees with the theoretical results. The small difference is numerical noise resulting from the different schemes used to solve the ordinary differential equations (Runge–Kutta versus Euler schemes).

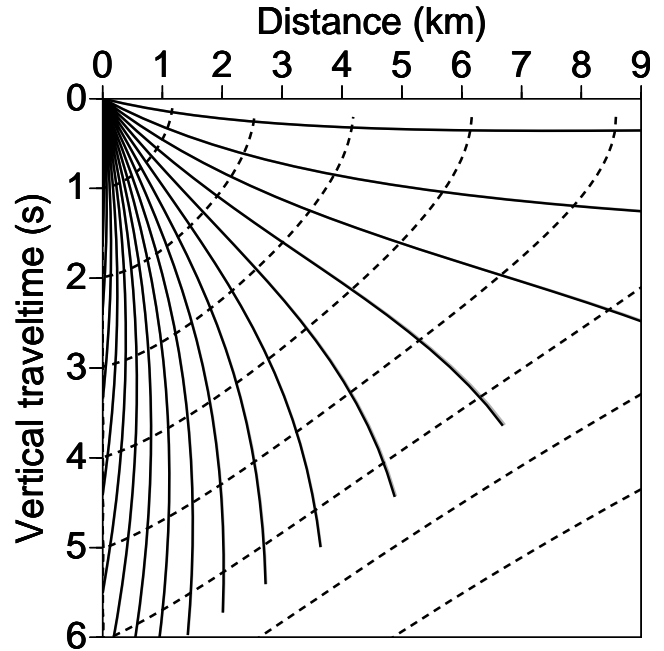


Figure 2. Ray paths and corresponding wave fronts in the $(x-\tau)$ -domain for an inhomogeneous VTI model with $v(x, z)=2+0.2x$ km s⁻¹ and $\eta(x, z)=0.1+0.05z+0.05x$. The black curves correspond to $v_v(x, z)=1.5+0.15x$ km s⁻¹ ($\alpha=0.75$) and the grey curves correspond to $v_v(x, z)=1.5+0.15x+0.75z+0.075xz$ km s⁻¹ ($\alpha(z)=0.75+0.375z$). In both cases, α is laterally invariant, and as a result the two curves overlap.

in the $(x-\tau)$ -domain coordinates and, as a result, the rays and corresponding wave fronts appear in the $(x-\tau)$ -domain. The vertical velocity varies considerably between the two models corresponding to the two sets of curves (black and grey), yet the curves coincide exactly. That is because in both models α , which is the ratio of the vertical to NMO P -wave velocity, does not vary laterally—a condition for the independence of ray tracing from vertical velocity in the $(x-\tau)$ -domain. Therefore, under this condition, ray tracing is dependent on only v and η .

However, when α varies laterally, ray tracing does depend on the vertical velocity. The amount of dependence is controlled by the size of the lateral variation in α . Fig. 3 shows rays penetrating in the same model as in Fig. 2, but with the grey curves corresponding to a laterally varying α that satisfies

$$\alpha(x, z) = \frac{(1.5 + 0.1x)(1 + 0.5z)}{2 + 0.2x}.$$

On the other hand, for the black curves, $\alpha=0.75$. For the laterally varying α model, at $x=0$ and $z=5$ km, $\alpha=2.625$, while at $x=5$ and $z=5$ km, $\alpha=2.333$. This big difference corresponds to a large variation in the ratio of the vertical to NMO P -wave velocity, a lot more than would be expected in practice. However, the differences in traveltimes between the two models are moderate. This fact implies that, despite the apparent influence of vertical velocity on ray tracing in the $(x-\tau)$ -domain coordinates when α varies laterally, such influence is small overall.

Assuming that δ , the parameter that relates the vertical and NMO velocities, ranges typically between -0.1 and 0.4 (this is a wide range; some studies have δ with a narrower range),

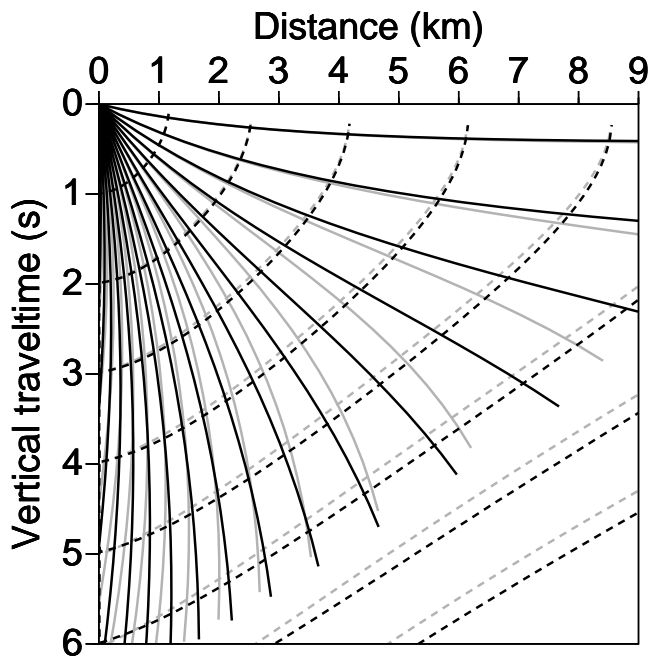


Figure 3. Ray paths and corresponding wave fronts in the $(x-\tau)$ -domain for an inhomogeneous VTI model with $v(x, z) = 2 + 0.2x \text{ km s}^{-1}$ and $\eta(x, z) = 0.1 + 0.05z + 0.05x$. The black curves correspond to $v_v(x, z) = 1.5 + 0.15x \text{ km s}^{-1}$ ($\alpha = 0.75$) and the grey curves correspond to $v_v(x, z) = 1.5 + 0.1x + 0.75z + 0.05xz \text{ km s}^{-1}$ [$\alpha(x, z) = [(1.5 + 0.1x)(1 + 0.5z)] / (2 + 0.2x)$]. While for the black curves α is laterally invariant, for the grey curves α varies laterally, and as a result, the black and grey curves no longer coincide.

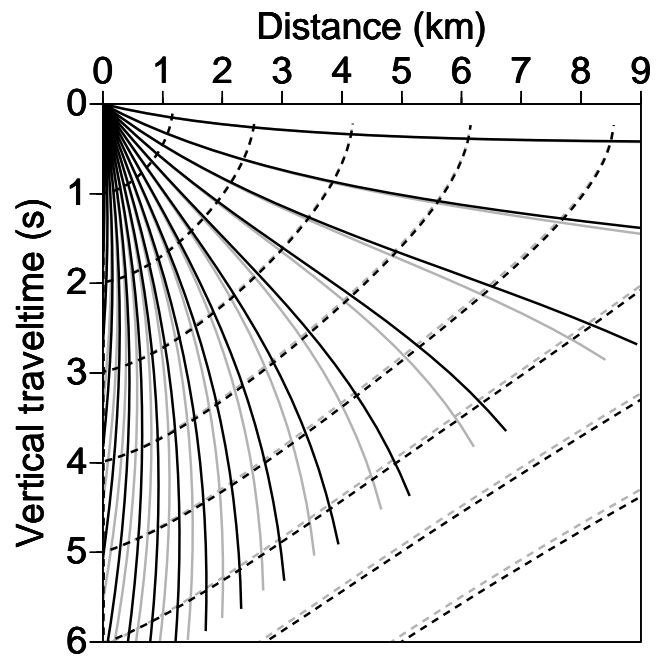


Figure 4. Ray paths and corresponding wave fronts in the $(x-\tau)$ -domain for an inhomogeneous VTI model with $v(x, z) = 2 + 0.2x \text{ km s}^{-1}$ and $\eta(x, z) = 0.1 + 0.05z + 0.05x$. The black curves correspond to $v_v(x, z) = 1.5 + 0.15x \text{ km s}^{-1}$ ($\alpha = 0.75$) and the grey curves correspond to $v_v(x, z) = 1.5 + 0.13x + 0.75z + 0.065xz \text{ km s}^{-1}$ [$\alpha(x, z) = [(1.5 + 0.13x)(1 + 0.5z)] / (2 + 0.2x)$]. Despite the fact that for the grey curves α varies laterally, the two curves are extremely close.

Fig. 4 shows a more practical α variation, in which the curves given by the two models are extremely close. The small variation suggests that for practical applications of the $(x-\tau)$ -domain coordinate processing, we can simply ignore the vertical velocity and rely on the NMO velocity and η for VTI media.

A LENS EXAMPLE

The presence of a lens anomaly in a velocity model results in a multi-pathing phenomena, the most interesting of which is the development of a triplication in the wave front. This multi-arrival traveltimes phenomenon typically occurs when a negative velocity anomaly is present. The intriguing issue is that triplication can also occur when we have positive η anomalies in a constant-velocity medium.

Fig. 5 shows rays and corresponding wave fronts that were obtained using conventional ray tracing in the depth domain (black curves) and using the equivalent ray tracing in the $(x-\tau)$ -domain (grey curves) through a VTI model with $\eta = 0.1$. The velocity model is shown in the background with a negative velocity anomaly that has a peak deviation of -1.0 km s^{-1} from the surrounding background velocity. The result is a noticeable triplication that develops soon after the rays pass the anomaly. Despite the triplication, the results of ray tracing in the two domains (depth and time) are similar.

Fig. 6 also shows ray paths through an anomaly. The anomaly is now in η , and it is positive. Therefore, in the background we display the η model, with $\eta = 0$ everywhere other than at the anomaly. Again, the black curves correspond to solutions

of ray tracing in the depth domain, while the grey curves correspond to ray tracing in the $(x-\tau)$ -domain. Triplication, smaller than that associated with the velocity perturbation, occurs in the wave front. Velocity-wise, this medium is homogeneous;

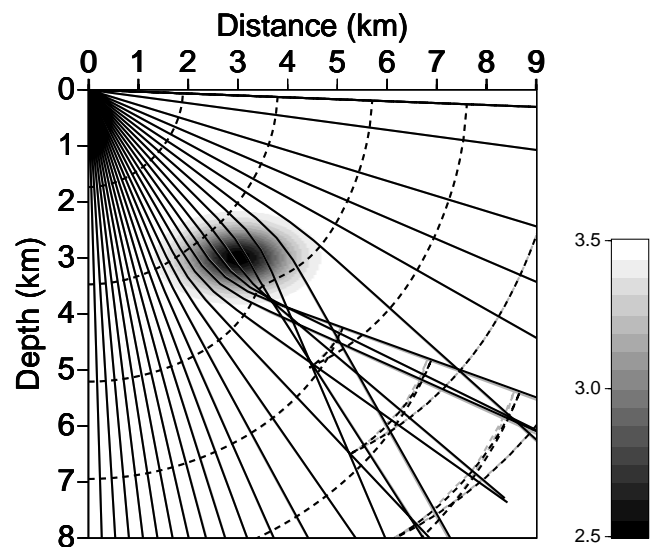


Figure 5. Ray paths (solid curves) and corresponding wave fronts (dashed curves) for an inhomogeneous VTI model, with $\eta = 0.1$. The rays are superimposed on the velocity model, given in km s^{-1} , of a negative velocity anomaly. The black curves are obtained through conventional ray tracing in the depth domain, and the grey curves are obtained using the equivalent $(x-\tau)$ -domain ray tracing, where the results are later converted to depth. The curves nearly overlap even in the presence of a triplication.

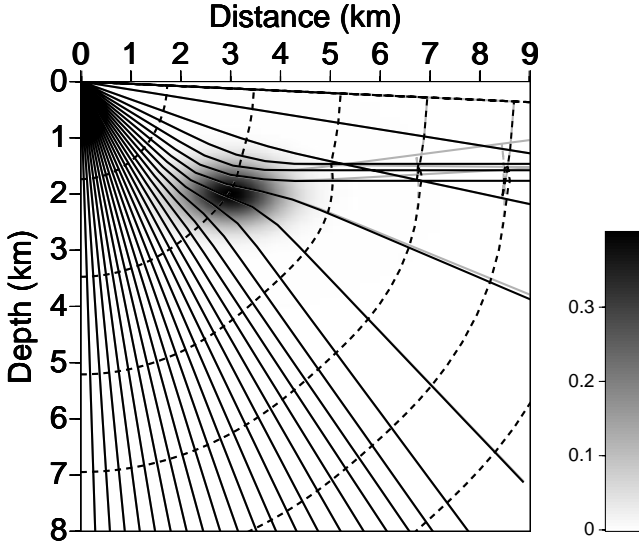


Figure 6. Ray paths and wave fronts for an inhomogeneous VTI model with $v=3.5 \text{ km s}^{-1}$. The rays are superimposed on the η distribution, which includes a positive η anomaly. The black curves are obtained through conventional ray tracing in the depth domain, and the grey curves are obtained using the equivalent $(x-\tau)$ -domain ray tracing, where the results are later converted to depth. The curves nearly overlap even in the presence of η -induced triplication.

it is η that is causing the severe bending of the rays. The rays with larger propagation angles from the vertical are the most influenced by the η anomaly.

FINITE DIFFERENCE SOLUTIONS OF THE $x-\tau$ WAVE EQUATION

In a general inhomogeneous medium, the finite difference method is the most practical method for solving the wave equation. Despite their enormous computational cost, finite difference schemes provide a comprehensive solution to the wave equation, which often includes an accurate representation of geometrical amplitudes.

In this example, we use the second-order acoustic wave equation for VTI media in the $(x-\tau)$ -domain, given by eq. (27), and therefore we need to solve simultaneously

$$\begin{aligned} \frac{\partial^2 P}{\partial t^2} = & -8 \frac{\partial^4 F}{\partial x^2 \partial \tau^2} v^2 \eta + \frac{\partial^2 P}{\partial x^2} v^2 (1 + 2\eta) - 16 \frac{\partial^4 F}{\partial x \partial \tau^3} v^2 \eta \sigma \\ & + 2 \frac{\partial^2 P}{\partial x \partial \tau} v^2 (1 + 2\eta) \sigma - 8 \frac{\partial^4 F}{\partial \tau^4} v^2 \eta \sigma^2 \\ & + \frac{\partial^2 P}{\partial \tau^2} [4 + v^2 (1 + 2\eta) \sigma^2] + f \end{aligned} \quad (28)$$

and

$$P = \frac{\partial^2 F}{\partial t^2},$$

where $f(x, \tau)$ is the forcing function. We use a second-order finite difference approximation for P -derivatives in eq. (28) and a fourth-order approximation for F -derivatives. The solution for elliptically anisotropic media is obtained by setting $\eta=0$.

Since Alkhalifah (2000) discusses, in detail, a finite difference application of a fourth-order equation that closely resembles this one, no detailed discussion is included here.

Fig. 7 shows a velocity model in depth (top) and its equivalent mapping in time (bottom). Fig. 8 shows the wavefield at 0.65 s resulting from a source igniting at time 0 s that corresponds to the isotropic velocity model in Fig. 7. The wavefield is computed using the finite difference approximations of eq. (26). The velocity model given in the $(x-\tau)$ -domain is the input velocity model in the finite difference application. This same velocity model is used to map the wavefield solution back to depth. The solid curve in Fig. 8 shows the solution of the conventional eikonal solver (Vidale 1990) implemented in the depth domain, and this curve nicely envelopes the wavefield solution. Therefore, computing the wavefield in the $(x-\tau)$ -domain and in the conventional depth domain are equivalent, regardless of the lateral inhomogeneity. However, the $(x-\tau)$ -domain implementation becomes independent of vertical P -wave velocity when $dx/dx=0$. It is also important to note that the apparent frequency of the time section is velocity-independent, while waves in the depth section have wavelengths very much dependent on velocity. This has important implications for grid sampling to avoid dispersion. Specifically, using the $(x-\tau)$ -domain finite difference wave equation, we are effectively scaling the vertical sampling to fit the velocity model so that the wavelength (normalized here) remains constant. Thus, we do not have to worry about the vertical velocity variation. This is convenient since the majority of the velocity variation in the subsurface is vertical.

CONCLUSIONS

We have derived an eikonal equation that describes the kinematics of wave propagation in the time domain. This eikonal equation provides exact traveltimes for a general

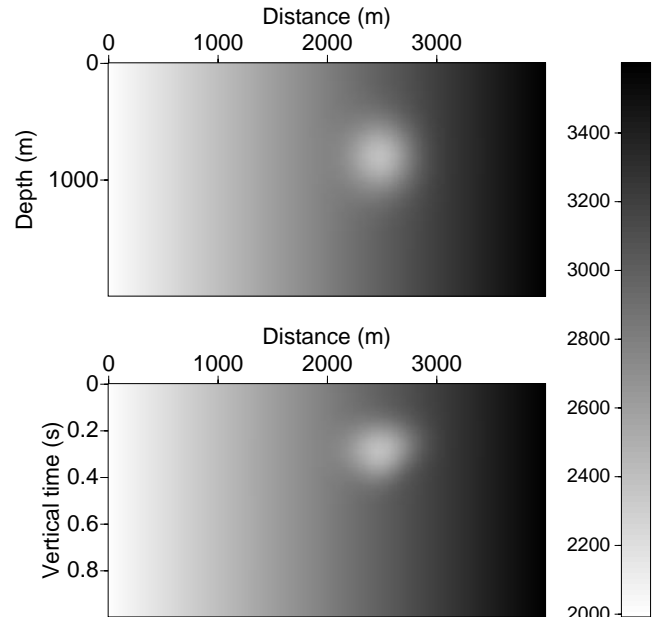


Figure 7. Velocity models in the conventional depth domain (top) and in the $(x-\tau)$ -domain (bottom). The velocity model includes a negative velocity anomaly perturbed from a background medium with $v(x)=2000+0.4x \text{ m s}^{-1}$.

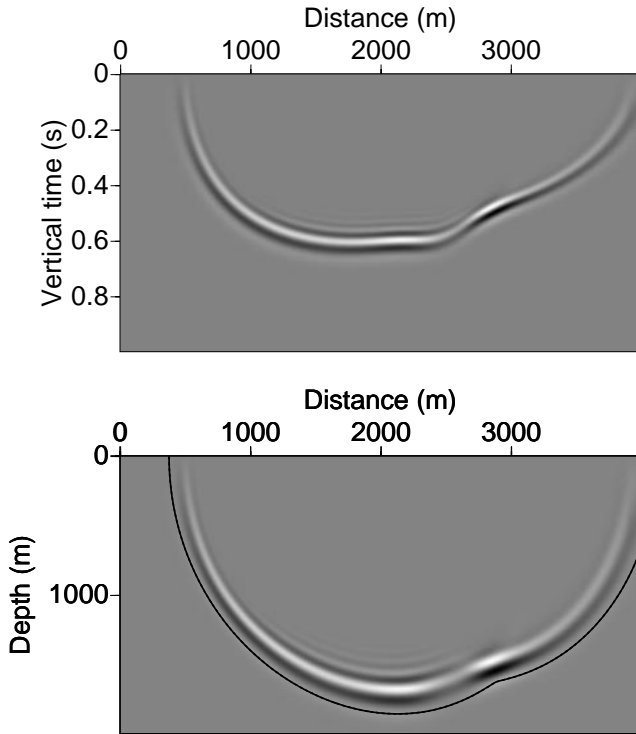


Figure 8. Top: the wavefield in the $(x-\tau)$ -domain at 0.65 s resulting from a source at distance 2000 m and $\tau=0$ for the isotropic velocity model shown in Fig. 7. Bottom: the same wavefield solution after mapping back to depth using the same velocity model. The black curve is the solution of the eikonal equation for the velocity model in Fig. 7 implemented using the conventional depth-domain eikonal solver.

inhomogeneous VTI, or isotropic, medium. One of its main features is its independence of the vertical P -wave velocity in VTI media, assuming that the ratio of the vertical-to-NMO velocity is laterally homogeneous, or in other words, that the anisotropy parameter δ does not change laterally. Even if δ varies laterally, the impact of the variation on traveltimes is generally small. As a result, for practical purposes, traveltime calculation in this new $(x-\tau)$ -domain is dependent on two parameters in VTI media and one in elliptically anisotropic media. Using the eikonal equation, we derive an acoustic wave equation that describes wave propagation in the $(x-\tau)$ domain. In summary, this paper establishes the basis for a full time-processing scheme in inhomogeneous VTI media that is dependent on only v and η , and independent of the vertical P -wave velocity.

REFERENCES

- Alkhalifah, T., 1998. Acoustic approximations for processing in transversely isotropic media, *Geophysics*, **63**, 623–631.
 Alkhalifah, T., 2000. An acoustic wave equation for anisotropic media, *Geophysics*, **65**, 1239–1250.
 Alkhalifah, T. & Tsvankin, I., 1995. Velocity analysis for transversely isotropic media, *Geophysics*, **60**, 1550–1566.
 Courant, R. & John, F., 1966. *Introduction to Calculus and analysis*, Interscience, New York.
 Hatton, L., Larner, K.L., Gibson, B.S., 1981. Migration of seismic data from inhomogeneous media, *Geophysics*, **46**, 751–767.

- Shearer, P.M. & Chapman, C.H., 1988. Ray tracing in anisotropic media with linear velocity gradient, *Geophys. J. Int.*, **94**, 575–580.
 Thomsen, L., 1986. Weak elastic anisotropy, *Geophysics*, **51**, 1954–1966.
 Tsvankin, I. & Thomsen, L., 1994. Nonhyperbolic reflection moveout in anisotropic media, *Geophysics*, **59**, 1290–1304.
 Vidale, J.E., 1990. Finite-difference calculation of traveltimes in three dimensions, *Geophysics*, **55**, 521–526.

APPENDIX A: THE STRETCH FACTOR IN TIME

In this appendix, we derive σ , given by eq. (6), in the $(x-\tau)$ -domain. Using such an equation allows us to avoid the process of mapping σ from depth to time and back. The vertical two-way traveltime, τ , is written as

$$\tau(x, z) = \int_0^z \frac{2}{v_v(x, \zeta)} d\zeta, \quad (\text{A1})$$

where z corresponds to depth. Similarly,

$$z(\tilde{x}, \tau) = \frac{1}{2} \int_0^\tau v_v(\tilde{x}, t) dt, \quad (\text{A2})$$

where \tilde{x} corresponds to the new coordinate system.

Using the chain rule,

$$\frac{\partial t}{\partial \tilde{x}} = \frac{\partial t}{\partial x} + \frac{\partial t}{\partial z} \beta, \quad (\text{A3})$$

where β extracted from eq. (A2) is given by

$$\beta(\tilde{x}, \tau) = \frac{\partial z}{\partial \tilde{x}} = \frac{1}{2} \int_0^\tau \frac{\partial v_v(\tilde{x}, t)}{\partial \tilde{x}} dt, \quad (\text{A4})$$

and the partial derivative in τ is

$$\frac{\partial t}{\partial \tau} = \frac{v_v}{2} \frac{\partial t}{\partial z}. \quad (\text{A5})$$

Therefore, the transformation from (\tilde{x}, τ) to (x, z) is governed by the following Jacobian matrix in two dimensions:

$$\mathbf{J}_c = \begin{pmatrix} 1 & \beta \\ 0 & \frac{v_v}{2} \end{pmatrix}. \quad (\text{A6})$$

The inverse of \mathbf{J}_c is

$$\mathbf{J}_c^{-1} = \begin{pmatrix} 1 & -2\beta \\ 0 & \frac{2}{v_v} \end{pmatrix}, \quad (\text{A7})$$

which should equal the Jacobian matrix for the transformation from (x, z) to (\tilde{x}, τ) , given by

$$\mathbf{J} = \begin{pmatrix} 1 & \sigma \\ 0 & \frac{2}{v_v} \end{pmatrix}. \quad (\text{A8})$$

As a result,

$$\sigma(\tilde{x}, \tau) = \frac{-2\beta}{v_v} = \frac{-1}{v_v(\tilde{x}, \tau)} \int_0^\tau \frac{\partial v_v(\tilde{x}, t)}{\partial \tilde{x}} dt,$$

which is a convenient equation, since we want to keep all fields, including the velocity field, in \tilde{x} - τ coordinates.

APPENDIX B: THE AMPLITUDE TRANSPORT EQUATION

To obtain the transport equation for this new (x - τ)-domain coordinate system, we use a ray-theoretical model of the image,

$$F(x, \tau, t) = A(x, \tau)f[t - \tilde{t}(x, \tau)],$$

as a trial solution to the wave equation (23). This procedure yields the eikonal equation as well as the transport equation that describes the amplitude behaviour, $A(x, y, z)$, of wave propagation. Substituting the trial solution into the partial differential equation (23) and considering only the terms with the highest asymptotic order (those containing the fourth-order derivative of F) yields the eikonal equation (9). The next asymptotic order (third order in derivatives of F) gives us a linear partial differential equation of the amplitude transport,

as follows:

$$\begin{aligned} & 2v^2 A_x (\tilde{t}_x + \sigma \tilde{t}_\tau) (1 + 2\eta - 8\eta \tilde{t}_\tau^2) \\ & + A[v^2 (1 + 2\eta) \sigma^2 - 8v^2 \eta (\tilde{t}_x^2 + 6\sigma \tilde{t}_x \tilde{t}_\tau + 6\sigma^2 \tilde{t}_\tau^2) \tilde{t}_{\tau\tau}] \\ & + 2A_\tau \{-8v^2 \eta \tilde{t}_x^2 \tilde{t}_\tau + v^2 \sigma \tilde{t}_x (1 + 2\eta - 24\eta \tilde{t}_\tau^2) \\ & + \tilde{t}_\tau [4 + v^2 (1 + 2\eta) \sigma^2 - 16v^2 \eta \sigma^2 \tilde{t}_\tau^2]\} \\ & + 4A + Av^2 \{2[\sigma + 2\eta \sigma - 8\eta \tilde{t}_\tau (2\tilde{t}_x + 3\sigma \tilde{t}_\tau)] \tilde{t}_{x\tau} \\ & + (1 + 2\eta - 8\eta \tilde{t}_\tau^2) \tilde{t}_{xx}\} = 0. \end{aligned} \quad (\text{B1})$$

Setting $\eta=0$ yields the corresponding transport equation for elliptically anisotropic media,

$$\begin{aligned} & 2v^2 A_x (\tilde{t}_x + \sigma \tilde{t}_\tau) + 2A_\tau [v^2 \sigma \tilde{t}_x + (4 + v^2 \sigma^2) \tilde{t}_\tau] \\ & + A[v^2 (\tilde{t}_{xx} + 2\sigma \tilde{t}_{x\tau}) + (4 + v^2 \sigma^2) \tilde{t}_{\tau\tau}] = 0. \end{aligned} \quad (\text{B2})$$

Both transport equations include first- and second-order derivatives of time with respect to position, calculated from the solution of the eikonal equation. Despite the apparent complexity of the transport equations, they are linear, and contain only first-order derivatives of A . As expected, amplitudes depend on second-order derivatives of traveltime or wavefront curvature. The dynamic ray-tracing equations behave similarly.